Materials Chemistry and Physics 132 (2012) 63–73

Contents lists available at SciVerse ScienceDirect

Materials Chemistry and Physics

journal homepage: www.elsevier.com/locate/matchemphys

Effect of processing technique on the transport and mechanical properties of graphite nanoplatelet/rubbery epoxy composites for thermal interface applications

M.A. Raza[a,*], A.V.K. Westwood[a], C. Stirling[b]

[a] Institute for Materials Research, University of Leeds, Leeds LS2 9JT, UK
[b] Morgan AM&T, Swansea SA6 8PP, UK

ARTICLE INFO

Article history:
Received 10 May 2011
Received in revised form 26 August 2011
Accepted 31 October 2011

Keywords:
Composite materials
Thermal conductivity
Electrical conductivity
Mechanical properties

ABSTRACT

Graphite nanoplatelet (GNP)/rubbery epoxy composites were fabricated by mechanical mixer (MM) and dual asymmetric centrifuge speed mixer (SM). The properties of the GNP/rubbery epoxy were compared with GNP/glassy epoxy composites. The thermal conductivity of GNP/rubbery epoxy composite (25 wt.% GNP, particle size 15 μm) reached 2.35 $W m^{-1} K^{-1}$ compared to 0.1795 $W m^{-1} K^{-1}$ for rubbery epoxy. Compared with GNP/rubbery epoxy composite, at 20 wt.%, GNP/glassy epoxy composite has a slightly lower thermal conductivity but an electrical conductivity that is 3 orders of magnitude higher. The viscosity of rubbery epoxy is 4 times lower than that of glassy epoxy and thus allows higher loading. The thermal and electrical conductivities of composites produced by MM are slightly higher than those produced by SM due to greater shearing of GNPs in MM, which results in better dispersed GNPs. Compression and hardness testing showed that GNPs increase the compressive strength of rubbery epoxy ~2 times without significantly affecting the compressive strain and hardness. The GNP/glassy epoxy composites are 40 times stiffer than the GNP/rubbery epoxy composites. GNP/rubbery epoxy composites with their high thermal conductivity, low electrical conductivity, low viscosity before curing and high conformability are promising thermal interface materials.

© 2011 Elsevier B.V. All rights reserved.

1. Introduction

Thermal management is a key aspect in electronic devices. Today it is possible because of VLSI technology to put thousands of transistors on a single silicon chip which is only a few microns in size and to build extremely complex structures and circuits on silicon chips. The problem becomes more severe due to miniaturization of electronics. As a result, large amounts of heat are generated in ever smaller spaces. Only efficient heat dissipation from microchips can ensure their fast and reliable operation. Continued growth of the industry at today's pace will be dependent upon improving electronic thermal management. Therefore, there is a strong demand for the electronics industry to devise and explore new thermal management systems which can overcome the challenges of heat dissipation of the present and future microelectronic devices [1–3].

Thermal interface materials (TIMs) are a vital component of modern electronic packaging. In electronics packaging, thermal interface materials are inserted between the chip (silicon die) and the heat spreader and between the heat spreader and the heat sink. TIMs reduce or eliminate the air gaps at the interface by conforming to the relatively rough and uneven mating surfaces and in this way overcome the thermal contact resistances at the interfaces [4]. The ability of TIMs to reduce the thermal contact resistance is strongly dependent on the high thermal conductivity of the TIMs [5]. However, high thermal conductivity alone does not guarantee that a material can be an efficient TIM as there are several other factors which govern the performance of TIMs [6]. These include spreadability, conformability, coefficient of thermal expansion, adhesion, surface roughness, etc. [7–9].

Current TIMs include thermal greases/pastes, solders, phase change materials and filled polymer matrices (polymer composites) including adhesives or gels. With the exception of solders, all other TIMs essentially contain thermally conducting fillers such as alumina, silica, boron nitride or aluminium nitride. These fillers are loaded into an organic matrix such as silicone oil or polyol ester oil to form thermal pastes or into polymers such as silicone, acrylic, or epoxy to form thermally conductive adhesives or gels [9–11]. Fillers are typically loaded into the matrix at 50–70 vol.% to achieve thermal conductivities in the range of 1–5 $W m^{-1} K^{-1}$ [12]. The selection of a TIM for electronics packaging depends on the gap between the surfaces. When the gap between the contacting surfaces is very

* Corresponding author. Tel.: +44 0113 343 2552; fax: +44 0113 246 7310.
E-mail addresses: mohsinengr@yahoo.com, pmmar@leeds.ac.uk (M.A. Raza).

0254-0584/$ – see front matter © 2011 Elsevier B.V. All rights reserved.
doi:10.1016/j.matchemphys.2011.10.052

small, usually TIMs with a thickness of 0.01 mm or less are required, ideally just thick enough to fill the valleys in the topography of the mating surfaces. Such types of TIMs include thermal greases and phase change materials. When the gap between the contacting surfaces is large, particularly when surfaces are not in direct contact, a TIM with a thickness of 0.1 mm or more is required for filling the gap. Such types of TIMs are called "gap filling materials". Polymer composites in the form of the tapes or thermal pads are recognized as gap filling materials [5,13]. Polymer composites for gap filling applications in electronics packaging require high thermal conductivity and conformability.

Carbon nanomaterials, including carbon nanotubes (CNT), graphite nanoplatelets (GNPs) and carbon nanofibers are attractive as TIM fillers due to their very high thermal conductivity. In current research, CNT are the most commonly chosen carbon filler material for TIMs. However, CNT-based TIMs have so far been unable to break into the commercial TIM market due to their low performance and high cost. Other factors which undermine the performance of CNT-based TIMs include difficulty in obtaining high filling ratios and in obtaining good dispersion in the matrix [11]. Graphite nanoplatelets (GNPs) are an emerging class of nanomaterials which are gaining favour for use in TIMs, compared to carbon nanotubes, due to their low cost. GNP is produced by the exfoliation of intercalated graphite at temperatures above 600 °C [14,15]. GNP is composed of one or more layers of graphene with a platelet thickness in the range of 0.3–100 nm and a very high aspect ratio. They exhibit a range of physical, chemical and mechanical properties. The single layered graphene sheet has in-plane thermal conductivity of 5300 W m^{-1} K^{-1} (estimated) [16] and a through-plane thermal conductivity of 3–6 W m^{-1} K^{-1} as compared to an axial thermal conductivity of 2900 W m^{-1} K^{-1} for a single wall carbon nanotube [14]. The in-plane thermal conductivity of GNPs is thus at least comparable to the carbon nanotubes [17] which makes them potentially very useful fillers for composite TIMs. The high in-plane thermal conductivity of GNP can be utilized in polymer composites either by orienting the GNPs (i.e., by making aligned composites) or by dispersing them randomly so that the GNPs form 3-dimensional networks in the matrix, either of which could lead to high thermal conductivity of the resulting composites. Several authors have proposed GNP-polymer composites for thermal management applications [12,16,18–20].

GNP/polymer composites have been developed by dispersing GNP in both thermoplastics [21–24] and in thermosetting polymers [25,26]. Thermoplastics are relatively conformable materials due to their low modulus, however, they have problems of creep and have high coefficients of thermal expansion which reduce the attractiveness of GNP/thermoplastic based TIMs. On the other hand, GNP/epoxy composites offer many advantages as TIMs. GNP can be dispersed easily into the low viscosity resins or curing agent. Epoxies have low coefficients of thermal expansion and have high thermal stability. Furthermore, they can be used as TIM adhesives for joining the mating surfaces and simultaneously play the role of thermal grease by filling the valleys of the mating surfaces before curing and can provide mechanical integrity to the package [27,28].

The properties of GNP/polymer composites strongly depend on good dispersion of GNPs [21,23]. After the exfoliation of intercalated graphite thin GNPs form but they tend to reagglomerate due to van der Waal's forces. Various methods of dispersion of GNPs into the polymers have been used to exploit the maximum benefits of thin GNPs. Kalaitzidou et al. [19] developed GNP/polypropylene (PP) composites by melt mixing using a twin-screw extruder followed by injection moulding. They reported that the resulting GNP/PP composite at 25 vol.% (40 wt.% of GNPs with an average particle size of 15 μm and 10 nm thickness) has a thermal conductivity of 1.5 W m^{-1} K^{-1}. Yu et al. [12] reported a thermal conductivity of 1.45 W m^{-1} K^{-1} (measured by steady state method) of GNP/epoxy composite at 5 vol.% of GNPs (∼10 wt.% of GNPs with particle size of 0.25 μm and 1.7 nm thickness). They produced composites by combined sonication and high shear mixing. Debelak and Lafdi [29] studied the effect of GNP particle size on the physical and mechanical properties of GNP/epoxy composites. They produced composites with particle sizes of 50, 100 and 150 μm by high shear treatment of exfoliated graphite in a solvent followed by ultrasonication. They reported that the GNP/epoxy composites at 20 wt.% of GNPs have thermal conductivity of 4.3 W m^{-1} K^{-1} (measured by laser flash method). They found that the thermal conductivity of the composites generally increases with increase of GNP particle size but surprisingly they found almost same thermal conductivity at 20 wt.% of GNPs for all particle sizes. Ganguli et al. [18] produced GNP/epoxy composites by an unconventional method using a Flaktex speed mixer which mixes filler and resin by dual asymmetric centrifuge action. The authors functionalised the surface of GNPs with 3-aminopropyltriethoxy silane and compared the thermal and electrical properties of functionalised and unfunctionalised GNP/epoxy composites. They reported that the functionalised GNPs increased the thermal conductivity (measured by laser flash method) of GNP/epoxy composite by 28-fold (GNPs having average particle size of 3.9 μm and 100 nm thickness) from 0.2 W m^{-1} K^{-1} (for the epoxy alone) to 5.8 W m^{-1} K^{-1} compared to a 19-fold improvement by unfunctionalised GNPs.

The research published on the GNP/epoxy composites has been totally confined to epoxy resins which are highly cross-linked, i.e. "glassy epoxies". They have very high stiffness and are inherently brittle in nature. In gel or adhesive TIM applications, the high modulus of glassy epoxy-based TIMs would not allow internal stresses to dissipate resulting in delamination of the epoxy from the surface [30]. Further, it is not possible to produce void free GNP/epoxy due to the difficulty in degassing these epoxies at higher loadings of filler with conventional techniques. Although these GNP/glassy epoxies have thermal conductivity above 4 W m^{-1} K^{-1}, they cannot be used as thermal pads or tapes due to their lack of conformability [8,31]. In the present paper, we put forward a solution to this problem of using GNP/epoxy composites for TIMs by replacing the glassy epoxy matrix with a rubbery epoxy matrix. The rubbery epoxy has a glass transition temperature around −35 °C and has very low stiffness [32]. Although it is not a true elastomer, its mechanical properties resemble one to some extent [32,33]. Furthermore, rubbery epoxy has very low viscosity before curing, fewer voids after curing and long workability before curing compared to glassy epoxy.

This paper reports the characterisation of GNP/rubbery epoxy composites produced by two processing techniques, namely conventional mechanical mixing (MM) and mixing by dual asymmetric centrifuge speed mixer (SM). The effect of GNPs wt.% and particle size on the viscosities of the dispersions before curing and on thermal conductivity, electrical conductivity, morphology and mechanical properties of the resulting composites are reported. The properties of GNP/rubbery epoxy composites are compared with GNP/glassy epoxy composites which were produced by identical techniques.

2. Experimental

2.1. Materials used

Graphite nanoplatelets (GNPs) were purchased from XG Sciences, Ltd. These GNPs were thin particles having a platelet morphology with reported thickness in the range of 5–10 nm. Particles with average size of 5 μm (GNP-5), 15 μm (GNP-15) and 20 μm (GNP-20) were used in this study. The GNP-5 and GNP-15 have very narrow size distributions with the majority of particles having sizes

of 5 and 15 μm, respectively. The GNP-20 has a broad particle size distribution and consists of a mixture of large and small particles.

Epoxy resin, Epikote 828, was kindly supplied by Hexion Specialty Chemicals and two aliphatic polyetheramine curing agents; Jeffamine D2000 and Jeffamine T403 (ex Huntsman Corporation) were used in this work.

Both rubbery and glassy epoxies were used as matrices for GNP/epoxy composites. The rubbery epoxy was produced by mixing epoxy resin, Epikote 828, and a curing agent, Jeffamine D2000, at weight ratios of 25:75, respectively. After curing the product is designated "rubbery epoxy" because it has a glass transition temperature below normal ambient temperature [33]. The glassy epoxy matrix, with T_g of ~80 °C, was developed by mixing Epikote 828 and Jeffamine T403 at weight ratios of 100:42, respectively.

2.2. Fabrication of composites

The GNP/epoxy composites were prepared by two mixing techniques. These are described in the following section.

2.2.1. Conventional mechanical mixing (MM)

For preparing samples with minimum dimensions of 40 mm × 25 mm × 10 mm, 40–50 g batches were prepared by mixing GNPs and epoxy. All of the composite dispersions were prepared at room temperature. GNPs were dried in an oven at 80 °C for a prolonged period to remove any moisture adsorbed on their surface. The dried GNPs were then mixed at appropriate percentages with rubbery epoxy resin by using a conventional mechanical mixer with a high speed motor and a propeller attached to a shaft. This was rotated in the mixture at 2500 rpm for 20 min, conditions which were identified, after various trials, as providing the most effective mixing; in that, increasing the mixing speed increases thermal conductivity (while reducing variability) but that above 2500 rpm the propeller becomes very unstable. After mixing, the batch was degassed under vacuum to remove any trapped air and was poured into a custom made aluminium mould. The filled mould was again degassed for half an hour to completely remove any trapped air. The GNP-5/Rubbery epoxy composites were prepared with a loading of 2–30 wt.% of GNP-5. The GNP-15/Rubbery epoxy composites were prepared with 2–25 wt.% of GNP-15. Loading of GNP-5 above 30 wt.% and GNP-15 above 25 wt.%, was found not to be feasible due to the high viscosity of the dispersion. The GNP-15/glassy epoxy composite was prepared with 20 wt.% of GNP-15. The curing treatment for GNP/rubbery epoxy and GNP/glassy epoxy was at 80 °C for 2 h and 120 °C for an additional 3 h. The samples of neat rubbery epoxy and glassy epoxy were also produced by MM method.

2.2.2. Mixing in a speed mixer (SM)

GNPs were mixed in the epoxy resin using a DAC 150 FVZ-K speed mixer. The DAC SpeedMixer™ works under the dual asymmetric centrifuge action which is achieved by the spinning of a high speed mixing arm in one direction while a cup containing the particles and resin (only) rotates in the opposite direction. This combination of forces in different planes enables extremely fast mixing.

The dried GNPs were mixed with rubbery epoxy at 3450 rpm for 10 min. These parameters were selected based upon the work of Ganguli et al. [18]. The dispersions of GNP/rubbery epoxy were degassed after mixing and then poured in to moulds and degassed for an additional 20 min. The curing schedule was the same as has been described for the composites prepared by MM. The GNP-5/rubbery epoxy composites were prepared by mixing the GNP-5 particles at 15 and 20 wt.% loading while GNP-15/rubbery epoxy composites were prepared by mixing the GNP-15 particles at 20 and 25 wt.% loading. GNP-20/rubbery epoxy composites were prepared at 2, 8, 12 and 15 wt.% loading and GNP-20/glassy epoxy composite was prepared with 12 wt.% of GNP-20.

2.3. Characterisation

2.3.1. Viscosity

The viscosities of the selected composite dispersions and pure rubbery epoxy were measured by rheometer (AR100 TA instruments). The flow test was performed using a parallel plate geometry having a diameter of 25 mm and a 500 μm gap between the plates. Stress was applied from 5 to 2000 Pa and shear rates up to 1–1000 s^{-1} were achieved. The data are reported as viscosity versus shear rate.

2.3.2. Thermal conductivity

Thermal conductivity of the neat epoxy and synthesised composites was measured by a hot disk [34] thermal constant analyzer (Hot Disk AB). For measurements, the sensor (C3891, radius 3.0 mm) was sandwiched between the two halves of the sample having flat surfaces each with thickness of about 8–10 mm and minimum x–y dimensions of 20 mm × 20 mm. The thermal conductivity of the samples was measured in a direction parallel to the direction of gravity that applied while the samples were left to settle/cure.

2.3.3. Electrical conductivity

For electrical conductivity measurement, cuboidal samples of the materials (~6 mm × 6 mm × 2 mm) were placed between two copper electrodes having dimensions slightly greater than those of the sample. The electrodes were connected to an Agilent mulitmeter which measured the resistance of the sample according to the two probe method which was deemed to be suitable owing to the relatively low electrical conductivity of the samples. To ensure the good contact between the sample and the copper electrode, samples were slightly compressed between the electrodes. To observe the effect of orientation of the GNP in the composites, the electrical conductivity of the samples was measured in directions parallel ($\sigma_{\parallel}$) and perpendicular ($\sigma_{\perp}$) to the force of gravity which applied during curing in the mould, respectively.

2.3.4. Scanning electron microscopy (SEM)

The morphology of the composites was observed using a using a Carl Zeiss LEO 60 mm 1530 field emission gun scanning electron microscope (FEG-SEM). The images were obtained using secondary electrons at 3 kV with a working distance of about 3.0 mm. The samples for SEM analysis were prepared by immersing strips of the composite, cut from the centre of moulded material, in liquid nitrogen for 10 min and then brittle-fracturing them in a vice. The fractured surface of the sample was sputter coated with a 5 nm thin layer of Pt/Pd alloys prior to the SEM analysis. All of the samples studied by SEM were sectioned in such a manner that one of the surfaces parallel to the direction of gravity during moulding was exposed for analysis.

2.3.5. Compression and hardness testing

Compression testing of neat epoxy and composites was carried out on an Instron universal testing system (Model no. 3382 with a 100 kN load cell). Cuboidal shaped samples (~8 mm × 8 mm × 10 mm) were compressed at a strain rate of 0.5 mm min^{-1}. The compression tests were performed on the samples so that compression occurred parallel to the direction of gravity in the original curing moulds. A typical compression test was carried out until the sample fractured. Hardness testing of the samples was done by a Shore hardness tester (Zwick) and values were measured on scale A.

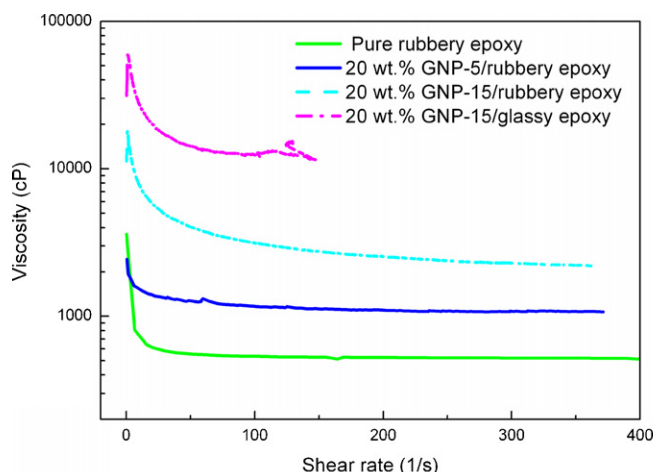

Fig. 1. Viscosity profiles of pure rubbery epoxy and GNP-epoxy dispersions before curing.

2.3.6. Thermogravimetric analysis

The GNP/rubbery epoxy composites were analyzed using thermogravimetric analysis (TGA) to determine their thermal stability. The test was performed (TA Instruments 'TGA 2050') by heating a cube-shaped 10 mg sample at a rate of 1 °C min^{-1} from 25 to 600 °C in a flow of N_2 at 10 ml min^{-1}.

3. Results and discussion

3.1. Viscosity

The plots of viscosity versus shear rate for pure rubbery epoxy and GNP-epoxy dispersions are presented in Fig. 1. It can be seen from Fig. 1 that, at the start of the test, the viscosities of pure epoxy and GNP/epoxy dispersions were very high. However, with a small increase of shear rate of about 10–15 s^{-1}, the viscosities dropped rapidly and then leveled off. The viscosity of pure rubbery epoxy resin is about 643 cP at a shear rate of 15 s^{-1}. The GNPs dispersed in either rubbery epoxy or glassy epoxy increased the viscosity of the dispersions at 20 wt.% loading. The viscosities of the 20 wt.% GNP-5/rubbery epoxy dispersion and 20 wt.% GNP-15/rubbery epoxy dispersion at shear rate of 15 s^{-1} are about 1432 cP and 6341 cP, respectively. The higher viscosity of the 20 wt.% GNP-15/rubbery epoxy dispersion is due to the larger particle size of GNP-15 compared to that of GNP-5. The large particles can reduce the free volume in the epoxy matrix and also undergo strong interaction with each other resulting in the increased viscosity of the epoxy dispersion. The viscosity of the 20 wt.% GNP-15/glassy epoxy dispersion is 23,171 cP at shear rate of 15 s^{-1}, which is about 4 times higher than the rubbery epoxy dispersion having an equivalent wt.% of GNP-15. It was not possible to continue the flow test for 20 wt.% GNP-15/glassy epoxy at higher shear rates due to the high viscosity of the dispersion. The increased viscosity of the glassy epoxy dispersion resulted because it contains 7 times more epoxy resin (Epikote 828) than the rubbery epoxy dispersion. The inherent viscosity of Epikote 828 is 11,000 cP which contributes to raising the overall viscosity of the glassy epoxy dispersions. The advantage of using the rubbery epoxy versus glassy epoxy is quite evident as the rubbery epoxy composition containing 20 wt.% of GNP-15 has a very low viscosity and this composition can be easily coated or dispensed by any processing technique used for the application of the thermal interface materials. We have found that GNP-5, GNP-15 and GNP-20 can be loaded into the rubbery epoxy at maximum loadings (to retain workability) of 30, 25 and 15 wt.%, respectively. Further higher loading of GNPs into rubbery epoxy was difficult. The GNP-20 has a broad particle size distribution compared to GNP-5 and GNP-15 as observed in the SEM (Fig. 2) and this lowers the maximum workable loading of GNP-20 particles. The small particles can occupy spaces between the large particles as well as in the resin and hence increase the viscosity. Therefore, it can be deduced that the loading of GNPs into epoxy is not only limited by the primary size of the particles but also depends on the particle size distribution. Ganguli et al. [18] reported the viscosity of a 20 wt.% exfoliated graphite/epoxy dispersion. This is about 1000 times higher than our 20 wt.% GNP-15/rubbery epoxy dispersion.

3.2. Morphology

SEM micrographs of fracture surfaces of the GNP/epoxy composites produced by SM and by MM are shown in Fig. 3a–j. Composites produced by MM and SM are not much different from one another with regard to morphology. Agglomerates of GNPs have thicknesses between 100 and 400 nm in the matrix as can be seen from Fig. 3. It can be seen from the low magnification images of 20 wt.% GNP-15/rubbery epoxy composites that GNPs are oriented in all directions with no apparent effect due to settlement under the force of gravity, as can be seen from the edges of the platelets which appear bright relative to the basal planes of the platelets (Fig. 3).

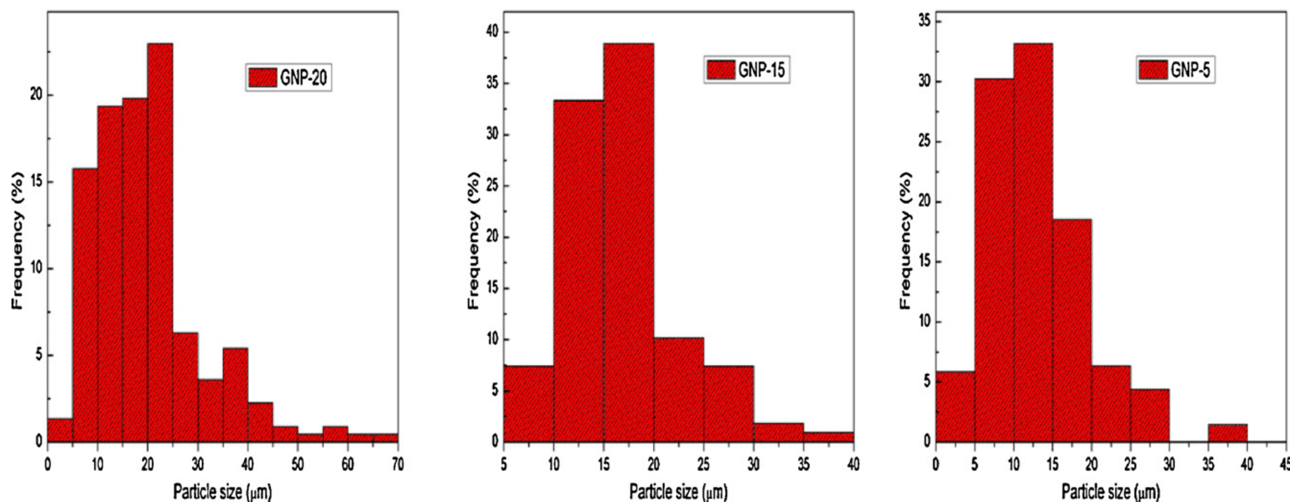

Fig. 2. Particle size distribution of GNP-20, GNP-15 and GNP-5 obtained on the basis of SEM analysis.

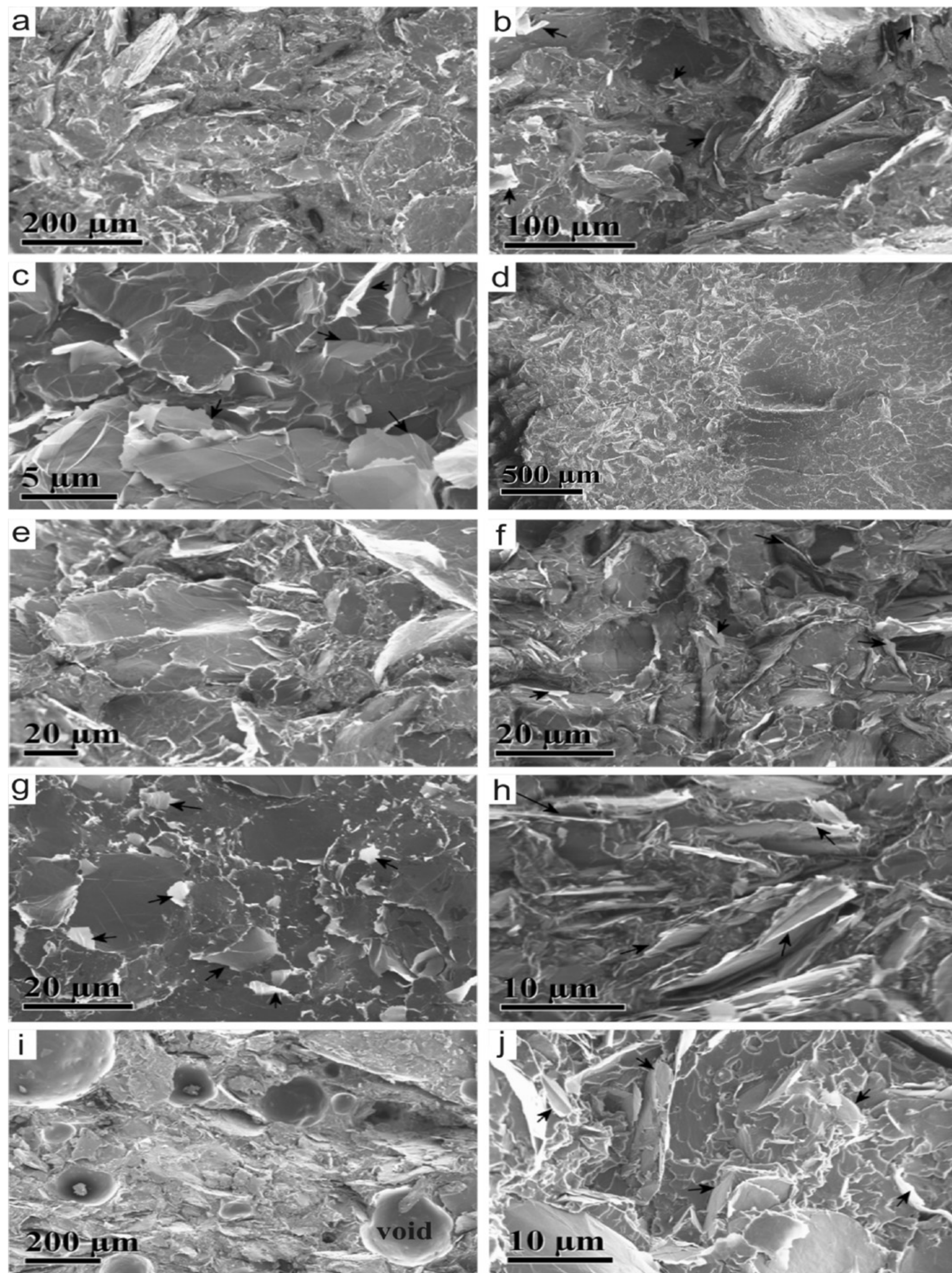

Fig. 3. SEM micrographs of 20 wt.% GNP-15/rubbery epoxy composite (a–c) produced by SM (d) 8 wt.% GNP-15/rubbery epoxy composite produced by MM, showing concentration gradient of GNP-15 (e–f) produced by MM (g–h) 30 wt.% GNP-5/rubbery epoxy composite produced by MM (i–j) 20 wt.% GNP-15/glassy epoxy composite produced by MM, (i) shows presence of voids (arrows pointing toward GNPs in the matrix).

Thus, the SEM analysis of GNP/rubbery epoxy composites showed that at 20 wt.% of GNP-15, GNPs are randomly oriented in the rubbery matrix resulting in an isotropic composite. However, in the case of the composite produced by MM at 8 wt.% loading of GNP-15, this has a significant concentration gradient in a 10 mm thick sample, as can be seen in Fig. 3d. This concentration gradient appeared due to the GNPs settling in the curing mould owing to low viscosity of the resin. This shows that at low loadings GNPs are not able to offer mutual hindrance to the setteling process. Most of the GNP-15 particles are touching each other which is an important requirement for the formation of the networks for thermal and electrical conduction. In contrast to the composite produced by MM, the composite produced by SM has thicker agglomerates of GNPs as can be seen from Fig. 3a–c. It appears that the SM was not able to break up the agglomerates of GNP effectively in comparison with mechanical mixing. The use of a propeller during MM might have produced high shearing effects which resulted in the deagglomeration of the GNP. The SEM images of the 20 wt.% GNP-15/glassy epoxy (Fig. 3i and j) showed that composite has many voids within it. This is because the high viscosity of the glassy epoxy dispersion did not allow trapped air to be removed completely under conventional vacuum degassing.

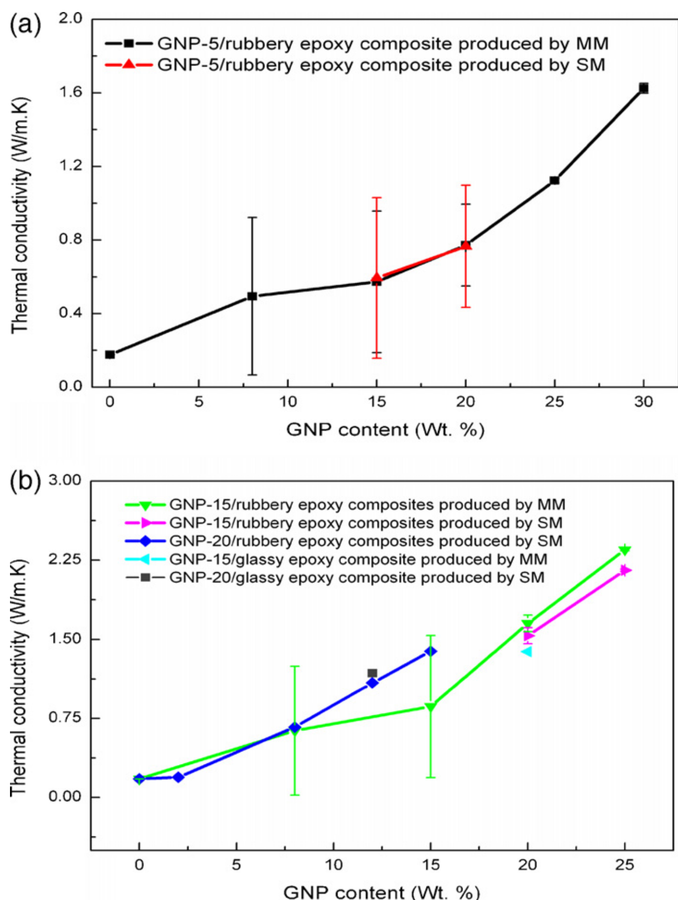

Fig. 4. (a) Thermal conductivity plot of GNP-5/rubbery epoxy composite as function of wt.% of GNPs produced by MM and SM process. (b) Thermal conductivity of GNP-15/rubbery epoxy produced by MM and by SM and GNP-20/rubbery epoxy composite produced by SM as a function of wt.% of GNPs with some corresponding data for glassy epoxy composites for comparison.

Table 1
Thermal conductivities of epoxies and GNP/epoxy composites.

Material	Fabrication method	Thermal conductivity, $W\,m^{-1}\,K^{-1}$	Standard deviation, $W\,m^{-1}\,K^{-1}$
Neat rubbery epoxy (RE)	MM	0.1769	0.0003
Neat glassy epoxy	MM	0.2256	0.0133
8 wt.% GNP-5/RE	MM	0.494	0.4281
15 wt.% GNP-5/RE	MM	0.5728	0.3848
20 wt.% GNP-5/RE	MM	0.7718	0.2227
25 wt.% GNP-5/RE	MM	1.1235	0.0120
30 wt.% GNP-5/RE	MM	1.625	0.0268
15 wt.% GNP-5/RE	SM	0.5938	0.4367
20 wt.% GNP-5/RE	SM	0.7652	0.3320
8 wt.% GNP-15/RE	MM	0.6346	0.6115
15 wt.% GNP-15/RE	MM	0.8625	0.6738
20 wt.% GNP-15/RE	MM	1.652	0.0778
25 wt.% GNP-15/RE	MM	2.35	0.0099
20 wt.% GNP-15/RE	SM	1.5345	0.0770
25 wt.% GNP-15/RE	SM	2.155	0.0099
2 wt.% GNP-20/RE	SM	0.1916	–
8 wt.% GNP-20/RE	SM	0.6665	–
12 wt.% GNP-20/RE	SM	1.088	–
15 wt.% GNP-20/RE	SM	1.388	–
12 wt.% GNP-20/glassy epoxy	SM	1.181	–
20 wt.% GNP-15/glassy epoxy	MM	1.385	–

3.3. Thermal conductivity

Plots of thermal conductivity of GNP-5/rubbery epoxy and GNP-15/rubbery epoxy composites (measured in a direction parallel to gravity that applied during curing in the mould) produced by MM and by SM processes as a function of wt.% of GNPs are presented in Fig. 4. The values of thermal conductivity of the developed composites and neat epoxies are presented in Table 1.

It can be observed from Fig. 4a and b that the thermal conductivity of the GNP/rubbery epoxy composites increases with the increase of both the wt.% of GNPs and the particle size of GNPs. The thermal conductivity of pure rubbery epoxy is $0.1769\,W\,m^{-1}\,K^{-1}$ and the thermal conductivity of the composites is higher than this at all wt.% loadings of the GNPs but there exists a very large standard deviation in the thermal conductivity of the composites produced at low wt.% of the GNPs as shown in Fig. 4. The standard deviation of thermal conductivity decreases with the increase of the wt.% of GNPs. In case of GNP-5, the standard deviation is very small at ≥25 wt.% loading in rubbery epoxy and in case of GNP-15 it is small at ≥20 wt.% loading. The large standard deviations resulted due to the presence of concentration gradients of GNPs in the 10 mm thick samples used for the measurement of the thermal conductivity by the hot disk method. The concentration gradient at low wt.% of GNPs developed due to the settling of GNPs into the epoxy resin owing to high density of the GNPs and low viscosity of the rubbery epoxy resin. Lower thermal conductivities were therefore measured when the sensor was sandwiched between upper cross-sections of the as cast sample compared to when the sensor was sandwiched between lower cross-sections of the as cast sample. The thermal conductivity of GNP-20/rubbery epoxy composites was only measured on lower cross-sections of the samples, therefore standard deviations are not reported. The thermal conductivity data show that the GNP/rubbery epoxy composites with homogeneous thermal conductivity can only be produced at wt.% higher than 15 in case of GNP-15 and at wt.% higher than 20 in case of GNP-5 particles, since at these, and higher, loadings the effects of settling are negligible, presumably because the filler particles hinder each other's movement under gravity.

Thermal conductivity of GNP-5/rubbery epoxy composites at 25 wt.% loading increases 6-fold to $1.123\,W\,m^{-1}\,K^{-1}$ and at 30 wt.% of GNP-5 the increase is 9-fold to $1.625\,W\,m^{-1}\,K^{-1}$, compared to the pure rubbery epoxy ($0.1769\,W\,m^{-1}\,K^{-1}$). Thermal conductivity increases for GNP-15/rubbery epoxy composite at 25 wt.% filler concentration to $2.35\,W\,m^{-1}\,K^{-1}$ – a 12 fold improvement compared to pure rubbery epoxy. Thermal conductivity of GNP-20/rubbery epoxy composite at maximum loading of 15 wt.% reached to $1.388\,W\,m^{-1}\,K^{-1}$ which is ~8 fold increase compared to pure rubbery epoxy. The thermal conductivity of 15 wt.% of GNP-20/rubbery epoxy composite is 10% lower than the thermal conductivity of 20 wt.% GNP-15/rubbery epoxy composite. Conversely, the superior thermal conductivity behaviour of GNP-20/rubbery epoxy composite at equivalent loading is attributed to the broad particle size distribution of GNP-20. Smaller particles can make bridges between the larger particles and hence create more conductive pathways. The thermal conductivity of 20 wt.% GNP-15/glassy epoxy composite (Fig. 4b) is $1.385\,W\,m^{-1}\,K^{-1}$ which is 16% lower than the equivalent rubbery epoxy composite ($1.652\,W\,m^{-1}\,K^{-1}$). The lower thermal conductivity of the glassy epoxy composite containing equivalent wt.% of GNPs can be attributed to the presence of a large number of voids in the final composite (Fig. 3i). However, the slightly higher thermal conductivity of 12 wt.% GNP-20/glassy epoxy composite produced by SM, as compared to the corresponding rubbery epoxy composites is attributed to the absence of void formation when lower loadings of GNPs are used with glassy epoxy. The neat glassy epoxy has 27.5% higher thermal conductivity than rubbery epoxy and we could expect higher thermal conductivity from GNP/glassy epoxy composite but the difference in thermal conductivity between the GNP/glassy and GNP/rubbery epoxy composite is negligible. Hence,

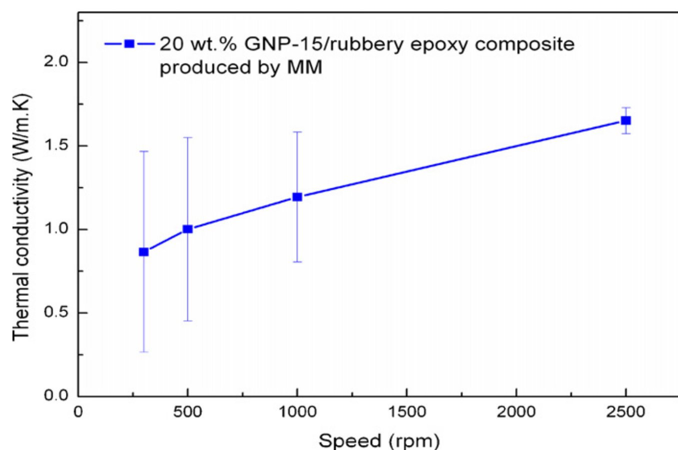

Fig. 5. Effect of mixing speed on the thermal conductivity of 20 wt.% GNP-15/rubbery epoxy composite produced by MM.

it can be deduced that the thermal conductivity of the composites mainly depends on the presence of the conducting networks formed by the particles and is less influenced by the inherent thermal conductivity of the matrix.

The particle size of GNPs plays a vital role in the thermal transport behaviour of the resulting composites. It is clear from the thermal conductivity data of the GNP/rubbery epoxy composites that at equivalent wt.% loadings, the thermal transport in composites with large particles is more effective than with small particles. In the case of large particles, fewer particles are involved in the formation of the conducting networks and hence there is reduced thermal resistance between the particles. The results suggest that by using the large size of the GNP particles, composites with similar thermal conductivity can be produced at relatively low wt.% of GNPs. The thermal conductivity plots as shown in Fig. 4 appear to have a transition point in the curves after which the thermal conductivity increases linearly with the increase of wt.% of the filler. For instance, the transition point in the case of GNP-15/rubbery epoxy composite appears to be at 15 wt.% of GNP (Fig. 4b). After this transition point, there are enough GNPs available so that they can orient themselves in the matrix in such a manner that they are touching each other and are able to form effective conducting networks as can be seen from SEM images of GNP/rubbery epoxy composites (Fig. 3e–h).

The thermal conductivities of GNP-5/rubbery epoxy composites produced by SM and MM are almost identical to each other while the thermal conductivity of GNP-15/rubbery epoxy composites produced by SM are slightly lower than the composites produced by MM. This slight decrease in thermal conductivity might arise due to presence of agglomerated GNP platelets in rubbery epoxy composites produced by SM, as can be seen from SEM micrographs of 20 wt.% GNP-15/rubbery epoxy composite(Fig. 3a–c). On the other hand, it appears that MM might be more effective than SM in breaking the agglomerates of GNPs to form thin GNPs.

The effect of mixing speed on thermal conductivity of 20 wt.% GNP-15/rubbery epoxy composites produced by MM for 20 min is presented in Fig. 5. The thermal conductivity increases with increasing mixing speed and the standard deviation in the value of thermal conductivity decreases as the mixing speed increases. The high standard deviation at low mixing speed shows that the GNPs are agglomerated and are not dispersed uniformly in the matrix. The standard deviations were obtained by measuring thermal conductivities on top and bottom cross sections of 10 mm thick samples. The thermal conductivity measured on top cross sections was significantly lower than bottom cross section which clearly shows the presence of concentration gradient in the composites produced at low speeds as discussed above (Fig. 3d). The agglomerated GNPs tend to settle more easily in the resin which resulted in a concentration gradient and thus large standard deviations. The high shear mixing achieved by the mechanical propeller at 2500 rpm helps break down the agglomerates of GNPs which results in uniform dispersion of the GNPs in the rubbery epoxy matrix and increased conducting network density in the matrix because many thin GNPs are available for development of conducting networks with high thermal conductivity ($1.652 \pm 0.078\,W\,m^{-1}\,K^{-1}$). It was found that the GNP/epoxy composites with the highest thermal conductivity values can be produced by MM at 2500 rpm with a minimum mixing time of 20 min. However, it should also be noticed that higher mixing speeds could also result in the breaking of the GNPs into smaller particles.

Ganguli et al. [18] reported a thermal conductivity of $4\,W\,m^{-1}\,K^{-1}$ for 20 wt.% exfoliated graphite/epoxy composite produced by speed mixer which represents a 19-fold increase compared to the pure resin. The exfoliated graphite used had lateral dimensions of 3.9 μm and thickness of 100 nm while the minimum particle size of the GNPs used in the present study was 5 μm and with thicknesses in the composites in the range of 100–400 nm. The epoxy used by Ganguli et al. [18] was glassy in nature. However, it is not easy to directly compare our GNP/rubbery epoxy composites with Ganguli's composites due to differences between the curing agents used. The use of different curing agents in epoxy systems can lead to different degrees of cross-linking and hence different properties. The thermal conductivity values of our GNP/rubbery epoxy composites are significantly lower than those reported by Ganguli et al. [18]. The thermal conductivity for 20 wt.% GNP-5/rubbery epoxy composite produced by SM was 5 times less than that of Ganguli's 20 wt.% exfoliated graphite/epoxy composite. Our composite preparation method is almost identical to that of Ganguli et al. but despite this our GNP/rubbery epoxy composites with slightly larger particle size, even at 30 wt.%, were unable to give the 19-fold improvement as obtained by Ganguli et al. The nature and process of exfoliation of graphite used to produce GNPs can also influence the thermal conductivity of the GNP/epoxy composite.

One main difference between our work and that of Ganguli et al. [18] is the thermal conductivity measurement technique. We measured the thermal conductivity using the hot disk method on as-cast samples having thickness of 8–10 mm or more while Ganguli et al. measured the thermal conductivity of the composites by laser flash method on 1 mm thick samples. Moreover, Ganguli et al. have not described the GNPs settling in the epoxy resin. Depending upon which regions of their samples were measured, it might be possible that the samples that they tested for thermal conductivity have unrepresentatively high concentrations of GNPs due to settling of graphite under gravity which resulted in overestimated values of thermal conductivity. Thus, the laser flash measurement might not be representative of the bulk thermal conductivity of the material. Debelak and Lafdi [29] reported the thermal conductivity of exfoliated graphite/epoxy composites for various particle sizes of exfoliated graphite (as mentioned in Section 1). They also used glassy epoxy for preparation of composites. The highest value of thermal conductivity in their work ($4.3\,W\,m^{-1}\,K^{-1}$) was achieved at 20 wt.% loading for all different sizes of exfoliated graphite in the epoxy. Debelak and Lafdi's finding [29] that the thermal conductivity of exfoliated graphite/epoxy composites increased with the increase of the filler content corresponds well to the thermal conductivity data reported for the various particle sizes of GNPs in our study. However, it is very strange that they found that the thermal conductivity values for all sizes of exfoliated graphite were almost the same at 20 wt.% loading. As for Ganguli et al. [18], Debelak and Lafdi [29] also used the laser flash technique for measurement of thermal conductivity but did not report the

existence of any concentration gradient effect due to graphite settling in the epoxy resins at low wt.% loadings.

3.4. Electrical conductivity

The electrical conductivity of GNP-15/rubbery epoxy composites as a function of wt.% of GNP-15 produced by MM and SM is presented in Fig. 6. The electrical conductivity of 20 wt.% GNP-15/glassy epoxy composites produced by MM is also presented in Fig. 6.

The electrical resistivity of pure rubbery epoxy in the cured state is very high and its exact value was not determined due to a limitation of the instrument, which has detectable range up to 100 MΩ. The electrical conductivity of composites at lower filler wt.% is not presented for two reasons: firstly, at lower filler concentration the electrical resistivity was not detectable due to the instrument limitation and secondly, due to the inhomogeneous settling effect of graphite at lower concentrations in rubbery epoxy, there were large variations in resistivity from one sample to another of same material.

The electrical conductivity of GNP-15/rubbery epoxy composites at 20 wt.% produced by MM is an order of magnitude lower when measured in the direction parallel to gravity than perpendicular to gravity that applied during curing of the composites. This shows that at 20 wt.% of GNP, despite the abovementioned inter-platelet hindering effect, there is still some tendency for the GNPs to orient their basal planes perpendicular to the direction of the force of gravity during curing. The electrical conductivity of 25 wt.% GNP-15/rubbery epoxy composite produced by MM is almost identical in the directions parallel and perpendicular to the gravitational force, indicating that the GNPs are randomly oriented in the matrix because, presumably, at this high concentration the inter-platelet hindrance is too significant to be overcome by gravity. The standard deviation in the values of the electrical conductivity are therefore very large for the 20 wt.% GNP-15/rubbery epoxy composites, as these are quite anisotropic, but are almost negligible for the more isotropic 25 wt.% GNP-15/rubbery epoxy composites produced by MM. The composite produced by SM has almost the same electrical conductivity to that produced by MM at 20 wt.% loading indicating the uniform distribution of the GNP into rubbery epoxy. However, the electrical conductivity of the 25 wt.% GNP-15/rubbery epoxy composite produced by SM is 4 orders of magnitude lower parallel to gravity and 3 orders of magnitude lower perpendicular to gravity compared to the equivalent composite produced by MM. This large difference shows that, in SM, GNPs are not subjected to sufficient shearing action to separate the agglomerated GNPs. The electrical conductivity data show the superiority of MM compared to SM in producing the GNP composites with effective electrically conductive networks. It can be deduced that the high electrical conductivity of 25 wt.% GNP-15/rubbery epoxy composite produced by MM is not only attributable to the high GNPs content but also to the dispersion of thinner GNPs into the rubbery matrix which helps to make effective conducting networks.

The GNP-5/rubbery epoxy composites were completely insulating even at loadings up to 30 wt.% of GNP-5. The GNP-20/rubbery epoxy composites were also electrically insulating up to 15 wt.% of GNP-20. Their electrical conductivity data are not reported because their resistances were more than the detectable range of the instrument.

The electrical conductivity of 20 wt.% GNP-15/glassy epoxy is almost 3 orders of magnitude higher in both parallel and perpendicular to the direction of gravity during curing compared to 20 wt.% GNP-15/rubbery epoxy composite. The significantly high electrical conductivity of glassy epoxy composites is attributed to the inherently lower electrical resistivity of glassy epoxy compared with that of rubbery epoxy. In contrast to the rubbery epoxy composite, the electrical conductivity of glassy epoxy composite parallel to the direction of gravity during curing is only slightly lower than in the perpendicular directions which indicates the formation of a quite isotropic GNP/glassy composite at 20 wt.% loading of filler.

Ganguli et al. [18] reported electrical conductivity that was 5 orders of magnitude higher for a 20 wt.% exfoliated graphite/epoxy composite than in the case of our 20 wt.% GNP-15/rubbery epoxy composites and 2 orders of magnitude higher than our 20 wt.% GNP-15/glassy epoxy composites. The large difference might be attributed to the type of epoxy matrix (based on curing agent) used as we have already seen the large differences between the electrical conductivities of rubbery and glassy epoxy composites. The electrical conductivity of GNP-based composites also reduces due to presence of heavily oxygenated, hydroxyl or epoxide functional groups on the basal planes of the GNPs or due to carbonyl or carboxylic group on the edges of the plane [21] due to the exfoliation process. In the work of Ganguli et al. and of Debelak and Lafdi, the variation of composites electrical properties with orientation of GNPs have not been assessed.

The electrical and thermal conductivity data of GNP/rubbery epoxy composites indicate that the electrical and thermal transport phenomena depend not only upon loading of GNPs but also on the particle size. Both the electrical and thermal conductivities of the composites significantly increase after a certain wt.% of GNPs is exceeded. For instance, GNP-15 at loadings greater than 15 wt.% into rubbery epoxy leads to substantial increases in electrical and thermal conductivity. However, in case of GNP-5, loadings up to 30 wt.% significantly enhance the thermal conductivity and yet failed to make the composites electrically conducting. The SEM images of 30 wt.% GNP-5/rubbery epoxy and 20 wt.% GNP-15/rubbery epoxy composites GNPs confirmed the likely presence of electrically conducting networks but despite this the electrical conducting behaviours of these composites are completely different. This shows that thermal conduction is not strongly dependent on particle size, unlike the electrical conduction. The highly electrically insulating behaviour of the 30 wt.% GNP-5/rubbery epoxy composite might result due to the more uniform dispersion of the GNP-5 in the rubbery epoxy matrix and its large interparticle distance, as observed by SEM (Fig. 3g and h), which reduces the effectiveness of the conducting networks required for electrical transport.

3.5. Compression testing

The uniaxial compression stress–strain diagrams of pure rubbery epoxy and GNP/rubbery epoxy (compressed in a direction parallel to gravity that applied during curing of the composites) composites are shown in Fig. 7.

The compression stress–strain curve of pure rubbery epoxy is typical of the stress–strain curve of an elastomer. It shows the softness and compliant nature of the rubbery epoxy. The addition of GNPs increases the compressive strength of the rubbery epoxy without impairing its compressibility. The GNP-15/rubbery epoxy composites experience a compressive strain of 10% at a stress of between 1.5 and 2 MPa, but further compression of GNP-15/composite requires ∼2 times higher stress to generate the same compressive strain as that of pure rubbery epoxy. There is a small decrease in compressive strength with the increase of GNP-15 content from 20 to 25 wt.%. This rather unexpected effect may be due to less efficient dispersion of the platelets at 25 wt.% loading. On the other hand, for otherwise equivalent composites, there is an increase in compressive strength for GNP-5/rubbery epoxy composite compared with GNP-15/rubbery epoxy composite. This behaviour can be explained by the fact that a smaller particle size can produce a stronger reinforcement effect than that from larger particles because there are more particles present in the

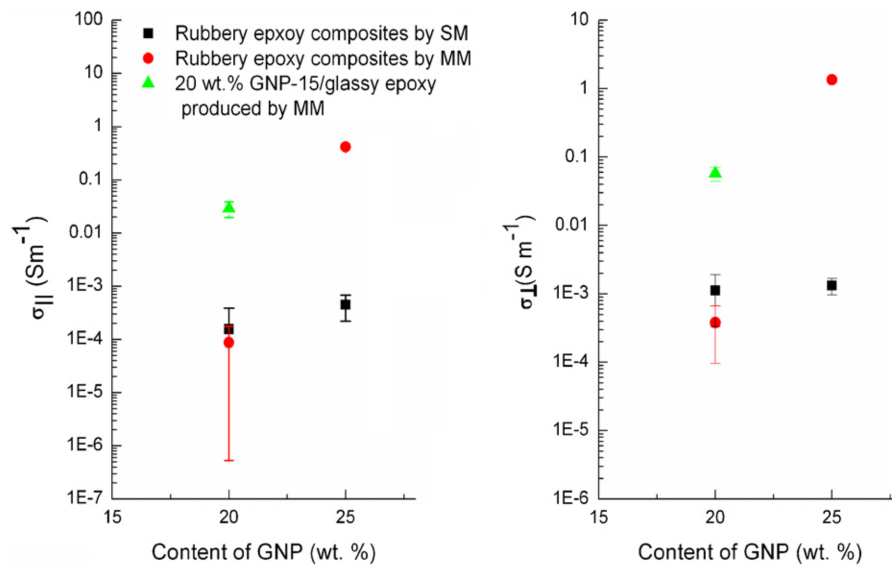

Fig. 6. Electrical conductivity of GNP-15/epoxy composites produced by MM and SM measured in the direction parallel and perpendicular to the direction of gravity that applied during curing in the moulds.

former case. The GNP-5 particles can thus form more interfaces with each other and with the resin. These interfaces can interact with one another during the process of deformation and hence lead to increase in the strength and reduction in compressive strain to failure of the composite. The compressive stress–strain curves of composites produced by MM and SM are almost identical to one another which indicate the uniform mixing of the GNPs into the rubbery matrix on macro-scale by both techniques. However, the slightly higher compressive strength and strain of composites produced by MM is attributed to the better dispersion of GNPs obtained by MM than SM. Overall increased compressive properties of GNP/rubbery epoxy composite might also be obtained due to some chemical interaction between GNP and rubbery epoxy. Previously, we [35] have reported in the case of GNP/silicone composites that compressive strength significantly decreases, which was attributed to the lack of interaction between GNP and silicone matrix. Thus, in the present case improved compressive properties suggest better chemical interaction between GNP and rubbery epoxy.

The comparison of compressive stress–strain curve of 20 wt.% GNP-15/rubbery epoxy and 20 wt.% GNP-15/glassy epoxy composites produced by MM is presented in Fig. 8. The glassy epoxy composite's stress–strain curve is similar to that of typical thermoset polymers, showing an extremely stiff and brittle nature. The high stiffness of the glassy epoxy composite is due to the high degree of cross-linking between the epoxy molecules. The glassy epoxy composite requires ∼40 times more stress to achieve the 10% compressive strain than the rubbery epoxy composite at equivalent GNP-15 loading. It can also be seen from Fig. 8 that the 20 wt.% GNP-15/glassy epoxy has very low compressive strength compared to the pure glassy epoxy. This is mainly due to the presence of plenty of voids in this composite as discussed in the Morphology section (Fig. 3i).

3.6. Hardness testing

The Shore hardnesses of pure rubbery epoxy, GNP-5/rubbery epoxy and GNP-15/rubbery epoxy composites produced by MM and SM are presented in Fig. 9. The hardness of pure rubbery epoxy increases with increasing wt.% of GNPs. The higher increase in hardness is caused by the addition of GNP-15 particles rather than GNP-5 particles. The hardness of GNP-15/rubbery epoxy

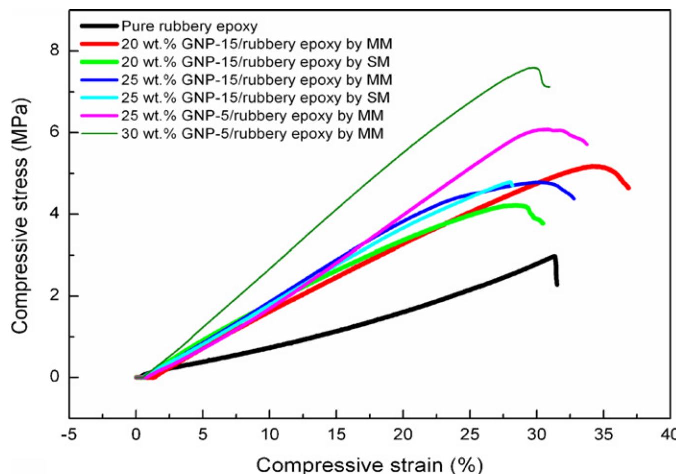

Fig. 7. Compression stress–strain curves of pure rubbery epoxy and GNP/rubbery epoxy composites.

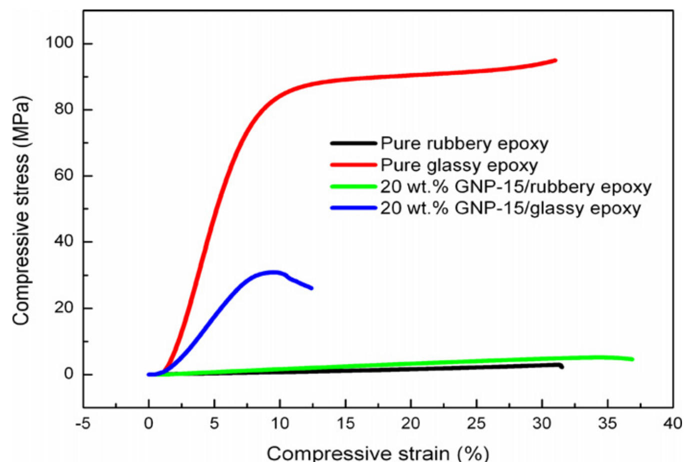

Fig. 8. Compressive stress–strain curve of pure rubbery epoxy, pure glassy epoxy, 20 wt.% GNP-15/rubbery epoxy and 20 wt.% GNP-15/rubbery epoxy composites produced by MM.

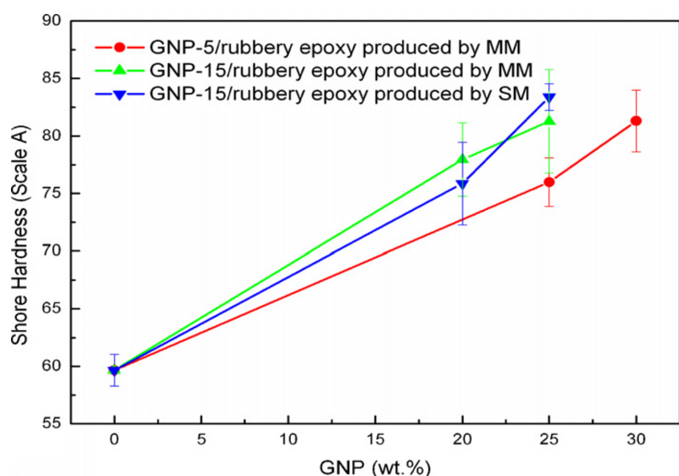

Fig. 9. Hardness of pure rubbery epoxy and GNP/rubbery epoxy composites.

upon addition of 25 wt.% GNP-15 increased by 36% from 59.66 to 81.27. The hardness of 25 wt.% GNP-15/rubbery epoxy composite produced by SM is slightly higher than corresponding composite produced by MM which might be due to the presence of agglomerates in the former. In the case of GNP-5/rubbery epoxy, a 36% increase in hardness is observed upon addition of 30 wt.% of GNP-5. There is not much difference between the hardness of the composites produced by MM and SM.

Overall, both transport and mechanical properties of composites produced by SM are slightly lower than the composites produced by MM up to 20 wt.% loading. However, at 25 wt.% loadings, composite produced by MM has significantly higher transport and mechanical properties than that produced by SM. The improved properties are attributed to the greater and uniform dispersion of GNPs in the matrix obtained by MM than SM. The use of propeller in mechanical mixing generates significant shearing effect at high speed which not only breaks agglomerates of GNPs but also thins them. Previously, we [35] reported that MM can produce GNP/silicone composites with better transport and mechanical properties compared to SM as it cannot only produce greater dispersion but can also produce thinner GNPs and the results of the present work are in good agreement with our previous work.

To date, the main criticism of epoxy-based thermal interface materials has been their high stiffness and brittle nature [8]. Stiff materials lack conformability, which makes it difficult for glassy epoxy type materials to develop good contact with bonding surfaces and high thermal contact resistance results at the interfaces. However, the compression and hardness testing of these GNP/rubbery epoxy composites showed that at the maximum possible loadings of GNPs in each case, these composites remain relatively soft and conformable materials in contrast to the glassy epoxy composites. Thus the use of rubbery epoxy as a matrix for filled polymer TIMs can increase their ability, as adhesives, to relieve stresses and thus overcome the problem of delamination. The use of rubbery epoxy also improves TIM conformability for thick gap filling applications, such as thermal pads. GNP/rubbery epoxy composites offer a promising alternative to glassy epoxy based thermal interface materials and so, overall, the high thermal conductivity, low viscosity before curing and conformable nature of GNP/rubbery epoxy composites make them promising as thermal interface materials.

3.7. Thermal stability of GNP/rubbery epoxy composite

The thermogravimetric analysis of 20 wt.% GNP-15/rubbery epoxy composites is presented in Fig. 10.

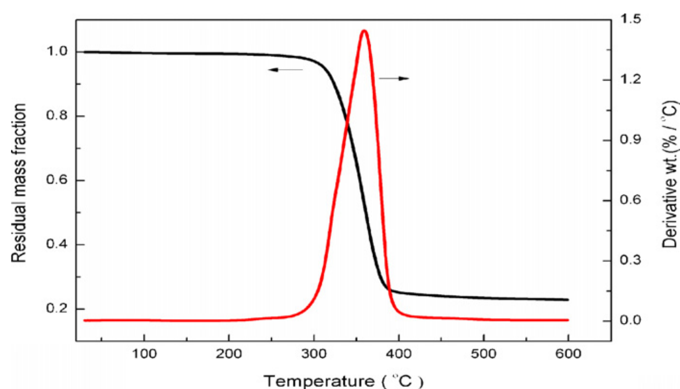

Fig. 10. Thermogravimetric analysis of 20 wt.% GNP-15/rubbery epoxy composite.

It can be observed from Fig. 10 that this GNP/rubbery epoxy composite is very stable up to a temperature of 250 °C because the total mass loss is less than 1%. Thus the GNP/rubbery epoxy composites are expected to be usable thermal interface materials as these are normally only required to work at operating temperatures below 125 °C. A mass loss of 10% occurred as the temperature reached 322 °C. Above this temperature mass loss occurred at a very high rate. The derivative mass change curve showed that rapid decomposition of the material took place at 358 °C.

4. Conclusions

- The GNP/rubbery epoxy dispersions are not workable once the wt.% of the GNP particles increases beyond a certain limit. The limit of loading for GNP-5, GNP-15 and GNP-20 that can be incorporated conveniently into rubbery epoxy by MM or by SM are 30, 25, and 15 wt.%, respectively. This limit varies depending on the particle size and particle size distribution of GNPs. It was not possible to produce GNP/rubbery epoxy composites at loadings lower than 15 wt.% in case of GNP-15 and 25 wt.% in case of GNP-5 with uniform thermal conductivity throughout the material due to the propensity of GNPs at low concentrations to settle under gravity owing to its high density in low viscosity rubbery epoxy dispersions.
- The thermal conductivity of GNP/rubbery epoxy composites increases with an increase in wt.% of GNPs and with the increase of particle size, as both of these factors favour establishment of improved thermal pathways. The thermal conductivity of GNP-5/rubbery epoxy composite (1.625 $\mathrm{W\,m^{-1}\,K^{-1}}$) increased by 9-fold compared to the pure rubbery epoxy (0.1795 $\mathrm{W\,m^{-1}\,K^{-1}}$) at 30 wt.% GNPs. The thermal conductivity of GNP-15/rubbery epoxy composite (2.35 $\mathrm{W\,m^{-1}\,K^{-1}}$) increased by 12-fold compared to pure rubbery epoxy at 25 wt.% loading of GNP.
- The thermal conductivity of GNP/rubbery epoxy composites strongly depends on the particle size distribution. In general, GNPs with a broad particle size distribution gave higher thermal conductivity than the particles with a narrow particle size distribution due to the availability of smaller particles which can bridge gaps between larger particles. It was found that the thermal conductivity of the composites produced by MM increases with increasing mixing speed and it is suggested that this might be due better dispersion of GNPs and probably formation of thinner GNPs upon more intense mixing.
- The thermal and electrical conductivities of the composites produced by SM are slightly lower than those of the composites produced by MM. This behaviour is attributed to increase shearing of GNPs in MM (cf. SM) which results in improved dispersion of GNPs.

- Compression and hardness testing of the GNP/epoxy composites showed that GNPs significantly increased the compressive strength to failure of rubbery epoxy. Compression testing showed that the GNP/rubbery epoxy composites, although they contain a very high wt.% of GNPs, retained good compliance, as they can be compressed by applying very small loads. GNP/rubbery epoxy composites produced by MM and SM are similar with regard to their mechanical behaviour.
- GNP/glassy epoxy composites have thermal conductivities that are slightly lower than the corresponding GNP/rubbery epoxy composite but the GNP/glassy epoxy composites are stiffer and have higher electrical conductivities than the corresponding GNP/rubbery epoxy composite.
- GNP/rubbery epoxy composites, with their high thermal conductivity, low electrical conductivity, low viscosity before curing, good thermal stability and high conformability meet the basic requirements of thermal interface materials and are promising candidates for thermal interface applications.

Acknowledgement

The authors thank Morgan AM&T and EPSRC for funding M.A.R.'s Dorothy Hodgkin Postgraduate Award Scholarship.

References

[1] A.L. Peterson, 40th Electronic Components and Technology Conference Proceedings, 1990, pp. 613–619.
[2] M. Mahalingam, Proceedings of the IEEE 73 (1985) 1396–1404.
[3] P.K. Schelling, L. Shi, K.E. Goodson, Mater. Today 8 (2005) 30–35.
[4] D.D.L. Chung, C. Zweben, Comprehensive Composite Materials (2003) 701–725.
[5] M. Grujicic, C.L. Zhao, E.C. Dusel, Appl. Surf. Sci. 246 (2005) 290–302.
[6] C. Lin, D.D.L. Chung, Carbon 45 (2007) 2922–2931.
[7] R. Prasher, Proceedings of the IEEE 94 (2006) 1571–1586.
[8] C. Lin, D.D.L. Chung, Carbon 47 (2009) 295–305.
[9] F. Sarvar, D.C. Whalley, P.P. Conway, IEEE 2006 Electronics System Integration Technology Conference, Dresden, Germany, 2006, pp. 1292–1302.
[10] D.D.L. Chung, J. Mater. Eng. Perform. 10 (2001) 56–59.
[11] J. Liu, T. Wang, B. Carlberg, M. Inoue, Electronics System-Integration Technology Conference 2 (2008) 351–358.
[12] A. Yu, P. Ramesh, M.E. Itkis, E. Bekyarova, R.C. Haddon, J. Phys. Chem. C 111 (2007) 7565–7569.
[13] C.-K. Leong, Y. Aoyagi, D.D.L. Chung, J. Electron. Mater. 34 (2005).
[14] B.Z. Jang, A. Zhamu, Journal of Materials Science 43 (2008) 5092–5101.
[15] Z.-S. Wu, W. Ren, L. Gao, B. Liu, C. Jiang, H.-M. Cheng, Carbon 47 (2009) 493–499.
[16] A.A. Balandin, S. Ghosh, W. Bao, I. Calizo, D. Teweldebrhan, F. Miao, C.N. Lau, Nano Lett. 8 (2008) 902–907.
[17] J.R. Potts, D.R. Dreyer, C.W. Bielawski, R.S. Ruoff, Polymer 52 (2011) 5–25.
[18] S. Ganguli, A.K. Roy, D.P. Anderson, Carbon 46 (2008) 806–817.
[19] K. Kalaitzidou, H. Fukushima, L.T. Drzal, Carbon 45 (2007) 1446–1452.
[20] H. Kim, A.A. Abdala, C.W. Macosko, Macromolecules 43 (2010) 6515–6530.
[21] S. Stankovich, D.A. Dikin, G.H.B. Dommett, K.M. Kohlhaas, E.J. Zimney, E.A. Stach, R.D. Piner, S.T. Nguyen, R.S. Ruoff, Nature 442 (2006) 282–286.
[22] G. Chen, J. Lu, D. Wu, Mater. Chem. Phys. 104 (2007) 240–243.
[23] T. Ramanathan, A.A. Abdala, S. Stankovich, D.A. Dikin, M. Herrera-alonso, R.D. Piner, D.H. Adamson, H.C. Schniepp, X. Chen, R.S. Ruoff, S.T. Nguyen, I.A. Aksay, R.K. Prud'homme, L.C. Brinson, Nat. Nanotechnol. 3 (2008) 327–330.
[24] F.T. Cerezo, C.M.L. Preston, R.A. Shanks, Compos. Sci. Technol. 67 (2007) 79–91.
[25] A. Yasmin, J.-J. Luo, I.M. Daniel, Compos. Sci. Technol. 66 (2006) 1182–1189.
[26] J. Li, P.-S. Wong, J.-K. Kim, Mater. Sci. Eng. A 1 (2008) 660–663.
[27] P. Kohli, M. Sobczak, J. Bowin, M. Matthews, Electronic Components and Technology Conference 51 (2001) 564–570.
[28] A. Prabhakumar, A. Zhong, S. Tonapi, D. Sherman, H. Cole, F. Schattenmann, K. Srihari, Electronic Components and Technology Conference (2003) 1809–1814.
[29] B. Debelak, K. Lafdi, Carbon 45 (2007) 1727–1734.
[30] R.S. Prasher, IEEE Transactions on Components and Packaging Technologies 27 (2004) 702–709.
[31] T. Lim, M. Velderrain, 9th Electronics Packaging Technology Conference, 2007, pp. 914–916.
[32] C. Gauthier, L. Chazeau, T. Prasse, J.Y. Cavaille, Compos. Sci. Technol. 65 (2005) 335–343.
[33] L. Liu, H.D. Wagner, Compos. Sci. Technol. 65 (2005) 1861–1868.
[34] S.E. Gustafsson, Review of Scientific Instrument 62 (1991) 797–804.
[35] M.A. Raza, A. Westwood, A. Brown, N. Hondow, C. Stirling, Carbon 49 (2011) 4269–4279.